

Use of a Pharmacophore Model To Discover a New Class of Influenza Endonuclease Inhibitors

Kevin E. B. Parkes,^{*,†} Philipp Ermert,[‡] Jürg Fässler,[‡] Jane Ives,[†] Joseph A. Martin,^{†,§} John H. Merrett,[†] Daniel Obrecht,[‡] Glyn Williams,[†] and Klaus Klumpp^{†,§}

Roche Discovery Welwyn, 40 Broadwater Road, Welwyn Garden City, Herts, AL7 3AY, UK, and Polyphor Ltd., Gewerbestrasse 14, CH-4123, Allschwil, Switzerland

Received July 30, 2002

Data from both our own and literature studies of the biochemistry and inhibition of influenza virus endonuclease was combined with data on the mechanism of action and the likely active site mechanism to propose a pharmacophore. The pharmacophore was used to design a novel structural class of inhibitors, some of which were found to have activities similar to that of known influenza endonuclease inhibitors and were also antiviral in cell culture.

Introduction

Influenza infects an estimated 120 million people in the US, Europe, and Japan in a typical year. It is a major cause of mortality as well as morbidity, particularly in children, the elderly, asthmatics, the immunocompromised, and diabetics. Vaccination with inactivated virus provides the most widely used method of prophylaxis, although it is not completely protective, particularly in the high-risk groups. Until recently the treatment options were limited to Amantidine or Rimantidine, which are only effective against influenza A, but have recently been enhanced by the launch of the neuraminidase inhibitors Relenza (zanamivir) and Tamiflu (oseltamivir phosphate). Nevertheless, there remains a need for improved treatment options.¹

Influenza virus is a segmented, negative-strand RNA virus. Synthesis of influenza virus mRNA occurs in the nucleus and is catalyzed by a virally encoded polymerase which consists of three subunits, PB1, PB2, and PA, which are highly conserved among all influenza virus strains. The polymerase complex contains an endonuclease function, which provides the polymerase with capped RNA primers for the initiation of transcription. In this unique and virus specific mechanism, capped and methylated host mRNAs bind to the polymerase and are cleaved by the endonuclease to form a 13-nt capped RNA primer with a free 3'-OH on which the nascent mRNA chain is assembled by the viral polymerase.² The endonuclease and polymerase active sites, which are responsible for primer formation and elongation, respectively, appear to be formed by distinct domains on the polymerase complex.³

The influenza endonuclease is an attractive antiviral target for a number of reasons:

(i) It is a key component of the viral transcription initiation mechanism, which has no cellular counterparts and should therefore provide good potential for discovering selective, nontoxic drugs.

(ii) Endonuclease inhibitors would complement existing influenza therapies since they are targeted to a different molecular target in the virus life cycle.

(iii) Due to the blockage of viral transcription, endonuclease inhibition is expected to have a virucidal effect. In contrast, the neuraminidase inhibitors do not prevent the formation of new virus particles, but interfere with virus release from the host cells and are therefore virustatic.

In this paper we present a novel pharmacophore or inhibitor binding model based on the biochemical characterization of the influenza virus endonuclease active site and the comparative analysis of selective endonuclease inhibitors. We also describe the use of this model to design a first library of compounds, and some refinements that were made to the model based on the biological results obtained with these compounds.

Results and Discussion

Biochemistry. DNA and RNA depolymerization and hydrolysis is central to a large number of replicative processes in cells, and three general mechanisms have been identified for enzymes involved in DNA or RNA hydrolysis. The first, which is specific to RNA hydrolysis, involves the intermediacy of a 2',3'-cyclic phosphate, and uses key protein residues which function as general acid and general base in a reversible phosphoryl transfer reaction.⁴ A second group of enzymes retain a key protein residue as a general base to activate the nucleophile, but also contain a single, catalytic metal ion in the active site. The pancreatic DNase I, the homing endonuclease I-PpoI, and Serratia endonuclease are examples of this group of enzymes.⁵ The final mechanism of phosphodiester bond cleavage is based on a set of two metal ions bound at 3.8–4.0 Å separation in the enzyme active site. The metal ions interact with the nucleophile, the leaving group, and a nonesterified oxygen to catalyze the phosphoryl transfer reaction. This last mechanism was originally developed from studies of the 3'-5' exonuclease domain of E. coli DNA polymerase I and alkaline phosphatase, but has since also been proposed for a number of other enzymes including DNA endonucleases, phosphodiesterases, and polymerases.⁶ As yet there is no three-dimensional

* Current address: Medivir UK Ltd, Peterhouse Science Park, 100 Fulbourn Road, Cambridge CB1 9PT, UK. kevin.parkes@medivir.com. Phone: ++ 44 (0)1223 271600, Fax: ++ 44 (0)1223 210514.

† Roche Discovery Welwyn.

§ Current address: Roche Palo Alto LLC, 3411 Hillview Ave., Palo Alto, CA 94304. joseph.martin@roche.com klaus.klumpp@roche.com.

‡ Polyphor AG.

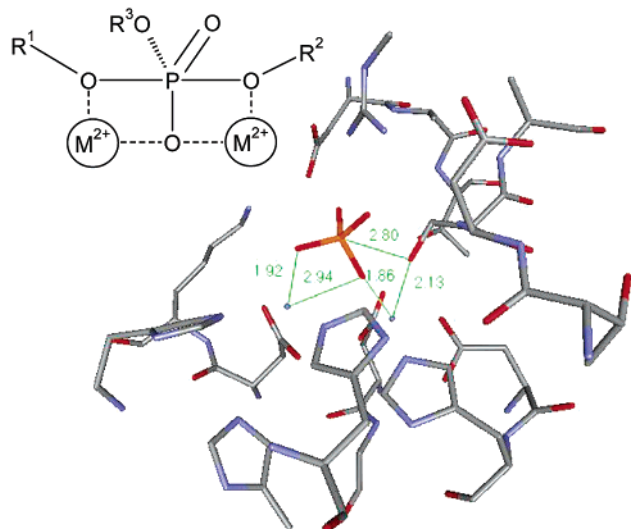


Figure 1. Active site structure of *E. coli* alkaline phosphatase^{6b} with the distances between the two catalytic metal ions and bound inorganic phosphate and the nucleophilic serine indicated. The metal ions are shown in blue (circles) and the inorganic phosphate molecule in orange. The inset depicts a schematic model of the phosphatase reaction transition state.

structure of the influenza virus endonuclease domain, and the primary sequence, although well conserved between different strains and isolates, shows little similarity with enzymes of known structure. However, studies by Klumpp et al.^{3b} have shown that (i) the endonuclease is activated by metal ions, particularly Mn^{2+} and Mg^{2+} ; (ii) the effect is cooperative, increasing supralinearly with concentration; and (iii) that a synergistic rate enhancement is seen with combinations of $Mn^{2+} + Mg^{2+}$, and $Mg^{2+} + Ni^{2+}$, strongly suggesting that the endonuclease activity of influenza polymerase belongs to the two metal ion group of phosphate-processing enzymes. Structures of several members of this family of enzymes have been reported,⁶ which together give a clear and consistent picture of the geometry of the interaction of the substrate phosphate and nucleophile or nucleofuge with the two active site metals. Based on the highly conserved structure of metal ion substrate interaction in this varied group of enzymes, a similar geometry can be reasonably hypothesized to apply also to the influenza endonuclease (shown in Figure 1 for the *E. coli* alkaline phosphatase 1alk^{6b}).

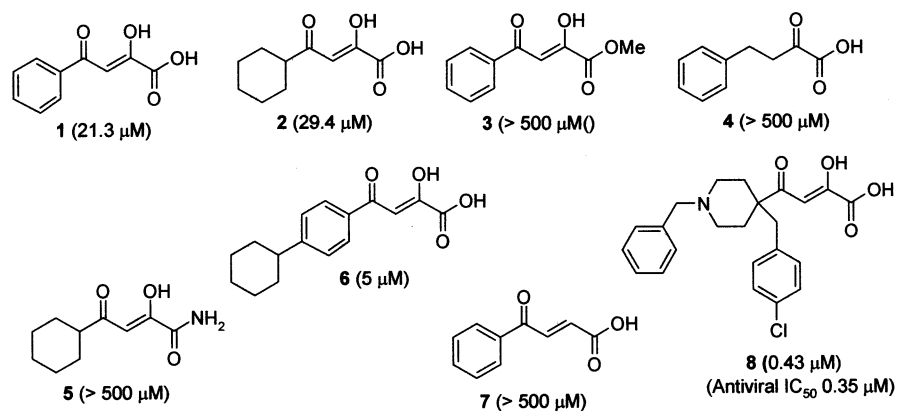


Figure 2. Diketobutanoic inhibitors of influenza endonuclease. Numbers in brackets denote IC_{50} values determined in the cap-dependent RNA polymerase assay with influenza A polymerase (**6**, **8**) or from literature.⁷

Influenza Endonuclease Inhibitors. The first reported inhibitors of influenza endonuclease were disclosed by workers from Merck who identified a number of 2,4-diketobutanoic acids (**1–8**) by high throughput screening for influenza polymerase activity.⁷ Their preliminary SAR studies demonstrated that the complete and unmodified diketobutanoic acid function was required for activity, although improvements in activity could be achieved by optimization of the phenyl ring (Figure 2). They also showed that these compounds specifically inhibited the endonuclease activity, had no effect on initiation or elongation of influenza virus mRNA synthesis, and were active in an in vivo mouse challenge model.⁸

Subsequently, the same group reported the isolation⁹ and synthesis¹⁰ of Flutimide (**9**), a fungal metabolite, that was also found to specifically inhibit the endonuclease function. They found that one of the isobutyl side chains could be replaced by a substituted benzyl moiety (**11**) and that analogues lacking the OH, or with protected OH groups, were inactive (**10**, **12**) (Figure 3).

Bristol-Meyers Squibb has reported a number of related, hydroxamic acid type inhibitors.¹¹ These compounds were also shown to be specific inhibitors of the endonuclease function although the activity of too few analogues was reported to allow any conclusions to be drawn about the SARs in the series.

N-Hydroxyimide Inhibitors. As a first step toward identifying a new class of endonuclease inhibitors we screened a targeted subset of the Roche compound library selected to include compounds with a range of potential metal-binding groups. From this screen we identified the *N*-hydroxyimide (**13**, Figure 4), which inhibited the endonuclease dependent influenza polymerase with an IC_{50} of 15 μM . The structure has similarities both to Flutimide (**9**) and to some of the inhibitors reported by the BMS group. Our preliminary structure activity studies are summarized in Figure 4 and demonstrate the absolute requirement for the *N*-hydroxy group and of the benzoyl carbonyl function (compounds **13**, **14**, **15**, and **16**). Unfortunately, attempts to prepare the direct analogue lacking the other carbonyl group were unsuccessful, although the inactivity of benzohydroxamic acid (**19**), and comparison of the heterocyclic analogues **17** and **18**, suggested that this carbonyl was also required for biological activity. Interestingly, the ring size was also critical with five- and

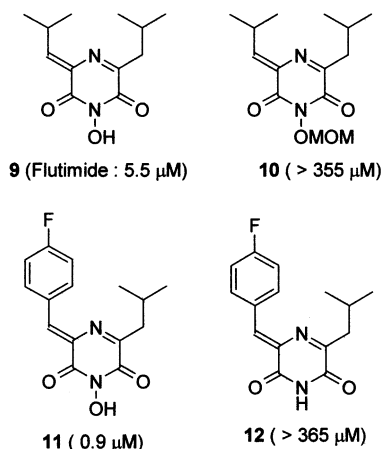


Figure 3. Flutimide and related inhibitors of influenza endonuclease. Literature IC_{50} values for the inhibition of influenza A RNA polymerase are shown in brackets.

seven-ring homologues (**20**, **21**, and **22**) showing no detectable activity despite the apparent conservation of the metal-binding *N*-hydroxyimide function.

Mode of Action. The inhibition of endonuclease dependent, mRNA primed polymerase activity by the prototypical *N*-hydroxyimide **13** was competitive with RNA, but noncompetitive with NTPs, consistent with the compounds binding to the endonuclease site (Figures 5a,b). In addition, endonuclease-independent, ApG-primed polymerase activity was not affected by the compound. This profile, which is essentially identical to that reported for the diketobutanoates, indicates that both compounds are specific inhibitors of the endonuclease activity of the influenza polymerase complex. We have also found that initial velocity reciprocal plots for the diketobutanoate **6** in the presence of varying concentrations of **13** were parallel, suggesting that the two classes of inhibitor are binding competitively at the same site (Figure 5c).

As mentioned above, the influenza endonuclease active site can be modeled as a two metal ion binding site. Therefore, some of the binding energy of the hydroxyimides and diketobutanoates could be derived from metal ion interaction in the active site, a binding mode supported by the mutually exclusive binding of the compounds to the enzyme. Further supportive evidence for this model came from the analysis of endonuclease inhibition in the presence of different metal ions. The endonuclease active site has been previously shown to accept a number of different metal

Table 1. Inhibition of Influenza Endonuclease by Diketobutanoate **8**

metal ion	IC_{50} [μM] ^a
Mg (II)	1.5
Mn (II)	0.012
Co (II)	0.031
Ni (II)	2.1
Fe (II)	0.6
Zn (II)	0.1

^a IC_{50} values were determined from the inhibition of endonuclease activity as determined from the analysis of reaction products on polyacrylamide gels using capped G20 RNA and influenza virus RNP as described previously.¹²

ions to catalyze RNA hydrolysis,^{3b,12} and interestingly, the inhibitory potency of the endonuclease inhibitors as illustrated by compound **8** was highly dependent on the type of metal ion used in the assay with the highest inhibitory activity being measured in the presence of Mn^{2+} or Co^{2+} (Table 1). This sensitivity to the metal ion used in the assay is consistent with a direct interaction between the oxygen atoms of the compound and the active-site metal ions.

Finally, measurement of the pH profile of the inhibitory potency of the diketobutanoate **8** showed a >50-fold increase in IC_{50} below pH 6.5 (Figure 6). This experiment indicated a key role for an ionized acidic function in the inhibitory process, but it does not allow one to distinguish between ionizations occurring in the inhibitor or in the active site. However, the pH at the transition between high and low inhibitory potency is similar to the reported second pK_a (7.62) for 2,4-diketo-4-(naphth-2-yl)butanoic acid¹³ and could suggest that these compounds were binding in a doubly ionized state. This is in apparent contrast with the hydroxyimides series which literature data suggests would be unlikely to be significantly singly ionized under the assay conditions (reported pK_a s for **13** are 8.0 and 11.9).¹⁴ For compound stability reasons we were not able to undertake the pH activity profiling of inhibitors from the *N*-hydroxyimide series, or measure the pK_a values of representative compounds from the two series ourselves under comparable, and preferably more physiological, conditions. However, we have observed by ¹H NMR that **13** was present as an equilibrium mixture of keto and enol forms in buffered aqueous solution, and that the equilibrium shifted significantly in favor of the enol tautomer on the addition of 50 mM Mg^{2+} . These results suggested that the two series may well have similar ionization profiles and certainly does not argue against building them into a single pharmacophore.

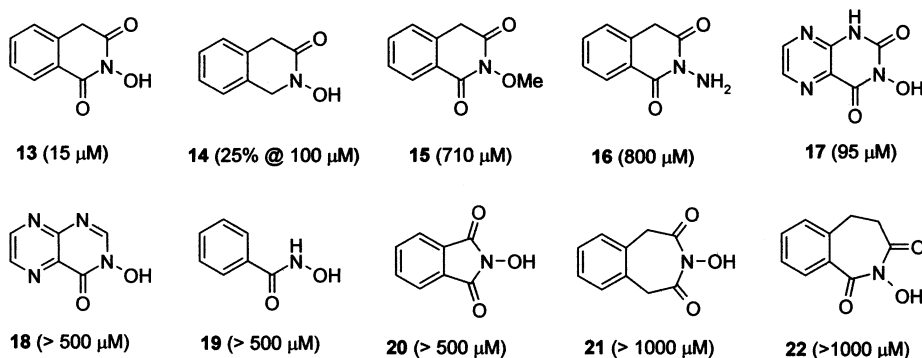


Figure 4. *N*-Hydroxyimide inhibitors of influenza endonuclease. Numbers in brackets denote IC_{50} values determined in the cap dependent RNA polymerase assay with influenza A polymerase (**13**–**16**; **19**–**22**) or from literature (**17**, **18**).¹¹

Table 2. Geometry and pKa Data Used in the Generation of the Pharmacophore Model

entry	compound class	$d(O1-O2)$, Å	$d(O2-O3)$, Å	$d(O1-O3)$, Å	pK _{a1}	pK _{a2}
1	diketobutanoic acids	2.65	2.75	5.17	~3.78 ^a	~7.62 ^a
2	<i>n</i> -hydroxyimides	2.71	2.71	4.64	8.0 ^b	11.9 ^b
3	alkaline phosphatase (1alk)	1.92	2.50	4.17	—	—
4	tetramic acids	2.68	2.88	5.23	?	?

See ref 13. See ref 14.

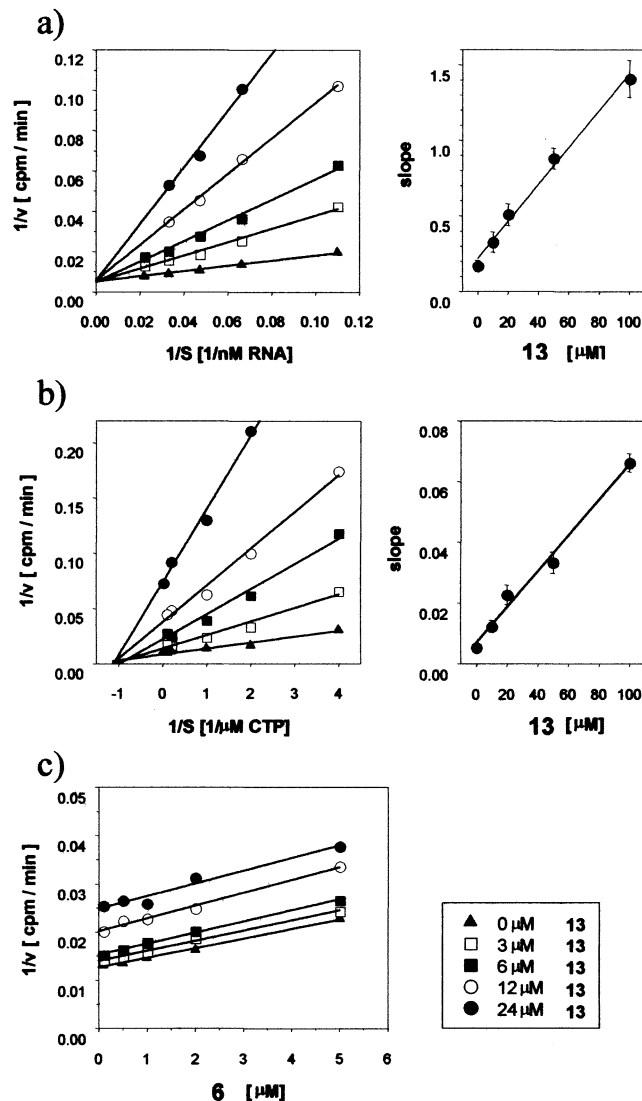


Figure 5. Inhibition of influenza polymerase cap-dependent transcription by *N*-hydroxyimide compound **13** is linear competitive with capped RNA and noncompetitive with nucleotide triphosphate substrates, consistent with compound binding to the endonuclease, and not to the polymerase active site. Influenza polymerase was incubated with variable amounts of AMV RNA substrate (a) or CTP (b) in the presence of 100 μ M (black circles), 50 μ M (white circles), 20 μ M (black squares), 10 μ M (white squares) **13**, or no compound (black triangles). $K_i = 14 \mu$ M, as determined from the replot of the slopes. (c) The binding of *N*-hydroxyimide **13** and diketobutanoate **6** to the influenza endonuclease binding site is mutually exclusive. Cap-dependent transcription activity was measured in the presence of increasing concentrations of **6** at defined concentrations of **13** as indicated. The observation of parallel lines in the Dixon plot indicates mutually exclusive binding of the two competitive inhibitors.¹⁷

Pharmacophore Generation. In both of the hydroxyimide and diketobutanoic acid classes of inhibitor, the SARs suggested that the oxygen functionality was

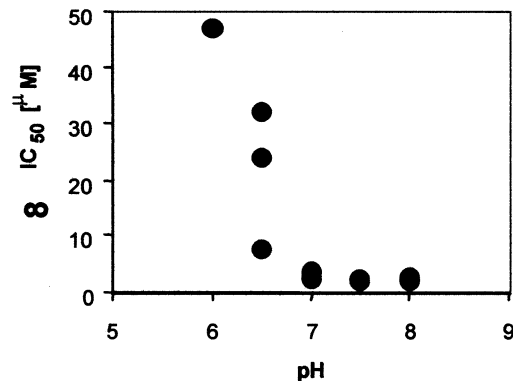


Figure 6. pH dependence of diketobutanoate **8** inhibitory potency. Dose–response curves were obtained for the inhibition of influenza polymerase cap-dependent transcription under different pH conditions. The inhibitory potency of **8** increased significantly with increasing pH, consistent with a critical deprotonation required for compound binding and endonuclease inhibition.

critical for activity. Closer examination reveals that the spatial arrangement of the oxygen atoms in the two classes of inhibitor was very similar (Table 2, entries 1 and 2). This similarity allowed a very plausible overlay of the two structures. Furthermore, we noticed that this arrangement of oxygen atoms was also quite similar to that of the phosphate oxygen atoms and nucleophilic serine oxygen atom complexing the two metal ions in the alkaline phosphatase structure (Figure 7). On the basis of this, and the observations described above, we propose a pharmacophore consisting of three oxygen atoms able to mimic the presumed interactions of the substrate, nucleophile, and leaving group oxygens in the transition state with the metal ions present in the active site of influenza virus endonuclease (Figure 8).

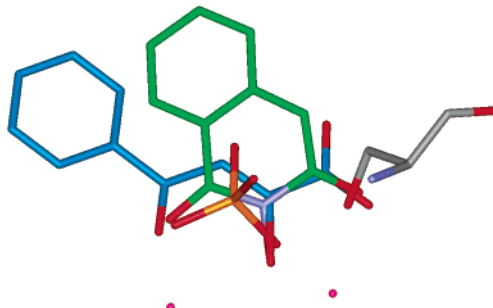
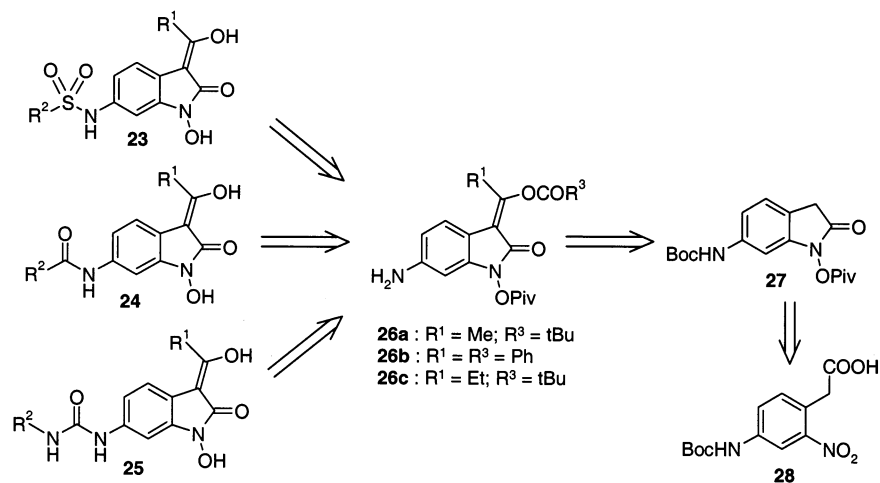


Figure 7. Overlay of 4-phenyl-2,4-diketobutanoate (**1**) and *N*-hydroxyhomophthalimide (**13**) with the inorganic phosphate, catalytic serine and metal ions of *E. coli* alkaline phosphatase.

This model allows us to rationalize the reported SAR for the diketobutanoic acid series and the Flutimide analogues as well as most of the results we obtained for the *N*-hydroxyimide class. However, the reasons why the five- and seven-ring homologues are inactive, despite

Scheme 1



apparently fitting the model, are unclear although several hypotheses can be advanced:

(i) In the case of **20** ring strain increases the hydroxy–oxygen to acyl–oxygen distance from 2.60 to 2.88 Å, resulting in a significantly less good overlay with the other inhibitors.

(ii) For both the five- and seven-ring analogues appreciable differences in ionization and tautomerization behavior would be expected. This would be most marked with the hydroxyphthalimide in which the second ionizable group is missing, but is also true for the ring-expanded analogues which due to their different ring conformations are likely to show different acidity and tautomerization behavior.

(iii) The seven-ring analogues are distinct in being nonplanar (modeling suggests for example that the phenyl ring of **21** would be bent 60.4° out of the imide plane) and may as a result make unfavorable contacts with the lipophilic binding region of the active site.

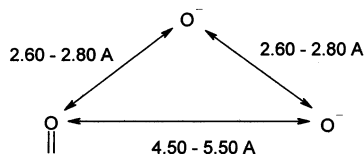
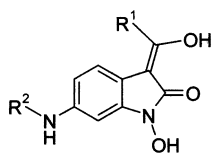


Figure 8. Proposed minimal pharmacophore for inhibitors of influenza endonuclease. The major feature of the model is a defined spacing of three oxygen atoms. One or two oxygen atoms may be ionized.

Inhibitor Design. Having found a potential pharmacophore can we use it to generate new leads? Unfortunately, the proposed pharmacophore relies on the correct spacing of three critical oxygen atoms with appropriate pK_a values and does not readily lend itself to an automated library searching approach to identify-



R¹ = Me, Et, Ph
R² = acyl (16), carbamoyl (15), sulfonyl (17)

Figure 9. Target tetramic acid library (see also Supporting Information, Table 4, for a list of synthesized compounds.

ing new core structures. We therefore generated a number of novel compound ideas and prioritized them, after modeling, on the quality of their alignment with the pharmacophore and their estimated pK_a values. This process eventually led to the selection of a functionalized tetramic acid (Figure 9 and Table 2, entry 4) for synthesis and biological evaluation. Since this first pharmacophore model did not take into account the contributions of the lipophilic regions of the compounds, we therefore chose to test the idea by designing the library of 144 compounds summarized in Figure 9, which included a range of substituents at both ends of the metal complexing functionality (Supporting Information).

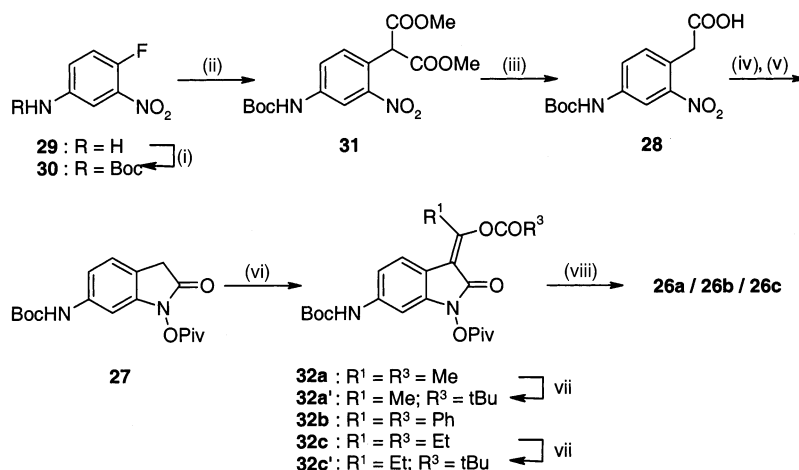
Synthesis. The synthesis of this library presented a number of challenges:

(i) *N*-Hydroxytetramic acid analogues of type **23**, **24**, and **25** had not been described in the literature and were expected to be highly polar and quite difficult to purify (Scheme 1).

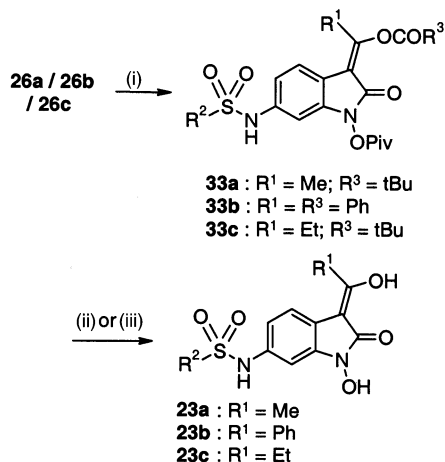
(ii) A suitable set of protective groups had to be found in order to allow a parallel synthesis approach with a simple deprotection protocol in the final step in order to facilitate isolation and purification.

As a result of a careful retrosynthetic analysis we identified the anilines **26**, in which the *N*-hydroxytetramic acid moiety is fully protected, as key intermediates (Scheme 1). Reaction of **26** with sulfonyl chlorides, acyl chlorides, or isocyanates would yield intermediates **33**, **34**, and **35**, respectively, which could easily be isolated and purified, before deprotection to give the final products. The key building blocks **26a**, **26b**, and **26c** should be available from the suitably protected indolinone **27**, which should in turn be available from the corresponding phenylacetic acid derivative **28**. Synthesis of 1-hydroxy-2-indolinones from the corresponding 2-nitro-phenylacetic acids has previously been described by Zn-reduction¹⁵ in low yield or by hydrogenation using Pt/C in ethanol and DMSO.¹⁶

The synthesis of the key building blocks **26a**, **26b**, and **26c** is depicted in Scheme 2. Commercial 4-amino-1-fluoro-2-nitrobenzene **29** was Boc-protected to give **30** in high yield using Boc₂O in THF at reflux. Reaction of **30** with 2.2 equiv of dimethylmalonate sodium salt in DMSO gave **31**, which after saponification and decarboxylation gave the key intermediate **28** in good yield.

Scheme 2^a

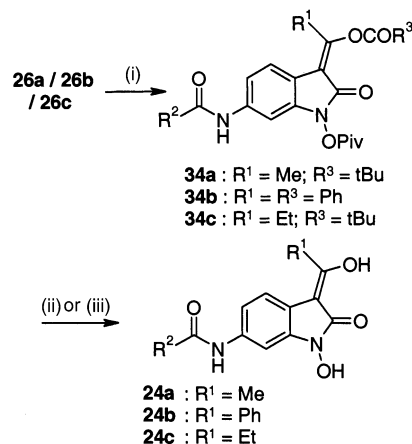
^a (i) : Boc₂O, THF, 80 °C; (ii) : CH₂(COOMe)₂, NaH, DMSO; (iii) : aq NaOH, MeOH, reflux; (iv) : Pt/C(5%), H₂, DMSO, EtOH; then AcOH; (v) : tBuCOCl, DIPEA, CH₂Cl₂; (vi) : R¹COCl or (R¹CO)₂O, DIPEA, DMAP; (vii) : tBuCOCl, pyridine, dioxane, NaCN or Bu₄NCN; v(iii) : HCl, dioxane or TFA, CH₂Cl₂.

Scheme 3^a

^a (i) : R²SO₂Cl, pyridine, DMAP, CHCl₃; (ii) : LiOH·H₂O, MeOH, THF, H₂O; then aq 1 M HCl; (iii) : *N,N*-dimethylaminopropylamine, CH₂Cl₂; then aq 1 M HCl and extraction with CH₂Cl₂.

Using a modification of the procedure of Kende et al.,¹⁶ we achieved selective hydrogenation of the nitro-group of **28** to the corresponding hydroxylamine intermediate using Pt/C (5%) in a mixture of ethanol and DMSO followed by in situ cyclization to yield the corresponding hydroxamic acid by addition of acetic acid. Although, the intermediate 1-hydroxyindolin-2-one derivative can be isolated and characterized, we preferred its direct conversion into **27** using pivaloyl chloride and DIPEA in CH₂Cl₂ since **27** is much more soluble and could be easily purified. The overall yield for the pivotal conversion of **28** into **27** was 50% even working on 50 g scale.

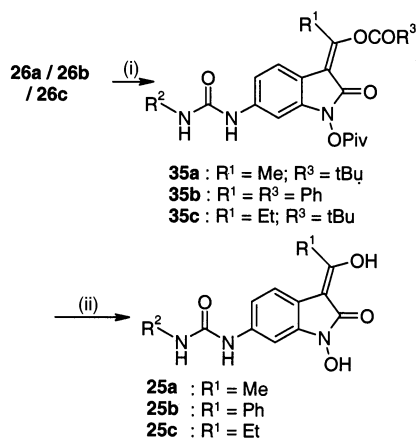
Following literature precedent¹⁶ for the Knoevenagel-type condensation of **27** with a carboxylic acid (R¹-COOH), in the presence of DMAP and *N,N*-dicyclohexylcarbodiimide, gave low yields of the corresponding *N*-pivaloyloxytetramic acid derivative. In addition, this product slowly reverted to **27**, suggesting that the Knoevenagel condensation may be reversible under these reaction conditions. However using R¹COCl or (R¹CO)₂O (2–4 equiv), DIPEA (3–5 equiv), and DMAP (10–20 mol %) in CH₂Cl₂ gave fairly good and reproducible yields (50–70%) of the intermediates **32** which could

Scheme 4^a

^a (i) : R²COCl, pyridine, DMAP, CH₂Cl₂; (ii) : LiOH·H₂O, MeOH, THF, H₂O; then aq 1 M HCl and extraction with CH₂Cl₂; (iii) : *N,N*-dimethylaminopropylamine, CH₂Cl₂; then aq 1 M HCl and extraction with CH₂Cl₂.

be isolated and purified by chromatography. For stability reasons, we preferred to convert the corresponding intermediates **32a** and **32c** into **32a'** and **32c'**, respectively, by reaction with pivaloyl chloride in a mixture of pyridine and CH₂Cl₂ in the presence of NaCN or tetrabutylammonium cyanide. The intermediates **32** were obtained as 3:1 to 2:1 mixtures of isomers, which can be separated by rather tedious column chromatography, although in general the isomers were not separated, as the final deprotection step yielded the same products. Removal of the Boc group was achieved by using 4 M HCl solution in dioxane, or TFA in CH₂Cl₂, at 0 °C, followed by extraction with saturated aqueous NaHCO₃ solution and CH₂Cl₂ to yield the key precursors **26a**, **26b**, and **26c**.

With the required building blocks in hand, we then turned to the library preparation. We found that the required sulfonamide or amide derivatives could be obtained by reaction with an acid chloride in a mixture of pyridine and CH₂Cl₂ in the presence of a catalytic amount of DMAP (Schemes 3 and 4). Final deprotection of **33** and **34** was achieved by reaction with LiOH·H₂O in a mixture of THF/MeOH (1:1) and subsequent

Scheme 5^a

^a (i) : R²NCO, CHCl₃ (ethanol free); (ii) : LiOH·H₂O, MeOH, H₂O, THF; then aq 1 M HCl.

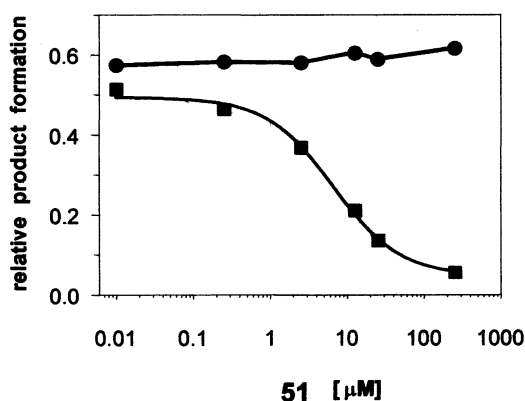


Figure 10. The tetramic acid **51** inhibits endonuclease, but not transcription initiation activity of influenza polymerase, as predicted by the pharmacophore model. Standard acrylamide gel based endonuclease and transcription initiation assays were performed in the presence of increasing concentrations of **51** and product bands were quantified by phosphorimager analysis. The dose response curves are shown for endonuclease (black squares) and transcription initiation from 11-mer capped primer RNA (black circles).

extraction with aqueous 1 M HCl solution and CH₂Cl₂ or even more conveniently by treatment with an excess of *N,N*-dimethylaminopropylamine in CH₂Cl₂ or dioxane and subsequent extraction with aqueous 1 M HCl solution and CH₂Cl₂ to yield **23** and **24** in both high yield and purity. The products could be further purified either by crystallization or reversed phase preparative HPLC.

The urea targets were conveniently accessed by reaction of precursors **26a**, **26b**, and **26c** with isocyanates in ethanol free CHCl₃ at temperatures ranging from room temperature to 80 °C (Scheme 5). Final deprotection was achieved using the LiOH procedure.

From a final library of 131 compounds, 26 members (**36–61**) were found to have significant inhibitory activity (IC₅₀ ≤ 50 μM) in the endonuclease dependent polymerase assay (Table 3). The most potent compound was **51**, with an IC₅₀ of 3 μM. Only five of the twenty-six active compounds (**36**, **37**, **38**, **48**, **51**) were tested against influenza B polymerase, and all showed significant cross-reactivity, suggesting a high degree of structural similarity in the active sites of influenza virus type A and B endonucleases. Of the six compounds (**36**, **37**, **38**, **45**, **48**, **51**) that were tested in cell culture, only

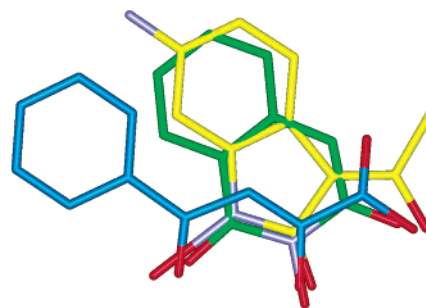


Figure 11. Initial overlay of the tetramic acid library core with 4-phenyl-2,4-diketobutanoate (**1**) and *N*-hydroxyhomophthalimide (**13**).

compound **36** showed significant antiviral activity (Table 3). We also confirmed with one of these compounds (**51**) that it is a specific inhibitor of the influenza polymerase endonuclease function in the gel-based endonuclease assay in agreement with the pharmacophore model. Compound **51** inhibited the endonuclease reaction with an IC₅₀ of 6.6 μM, but did not inhibit transcription initiation from an 11-mer capped primer RNA up to a concentration of 500 μM (Figure 10), and also showed no inhibition at 500 μM in the cap-independent polymerase assay.

Model Refinement. With no knowledge of the lipophilic regions of the binding site, the alignment of inhibitors onto the pharmacophore involved a degree of uncertainty since, if the tentative p*K*_a requirements of the atoms are neglected, the arrangement of the oxygen atoms is symmetric and would allow each inhibitor to be added to an overlay in either of two possible orientations. In the absence of other information the only way to select a preferred alignment is by selecting the overlay in which the hydrophobic regions of the inhibitors occupy the smallest total volume, thereby avoiding making unjustified assumptions about the extent of the lipophilic binding pocket. In neither of the two possible alignments of the hydroxyimides and diketobutanoates do the aromatic regions overlap, and the working alignment therefore had to be based on estimated p*K*_a values. Our initial addition of the tetramic acids to this alignment was chosen to minimize the lipophilic volume by overlapping its aromatic ring with that of the *N*-hydroxyimide (Figure 11). However, the biological results showed a clear preference for active compounds to have R¹ = Ph rather than Me or Et. This result suggested an improved alignment of the tetramic acid and diketobutanoic acid series in which the R¹ phenyl overlaps with the aromatic group of the diketobutanoates fulfilling both the p*K*_a and lipophilic volume requirements (Figure 12). It should be noted that the observed SAR within the tetramic acid series and the adjusted alignment with the diketobutanoates would also be consistent with the alternative orientation of the *N*-hydroxyimides (Figure 13). This alternative overlay would superimpose the *N*-hydroxyimide aromatic ring with that of the annelated tetramic acid aromatic ring. Further work will be required to test this possibility.

Conclusion

In summary, we have developed a pharmacophore model to explain the interaction of compounds with the influenza endonuclease active site based on the bio-

Table 3. Inhibitory Potencies of Tetramic Acid Compounds

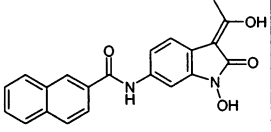
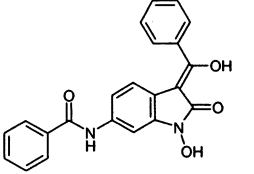
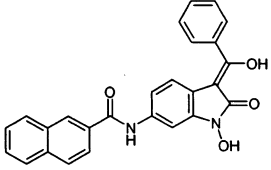
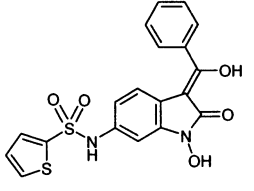
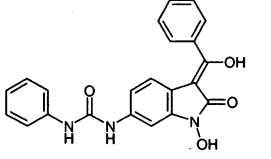
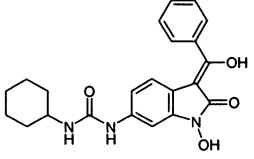
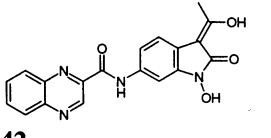
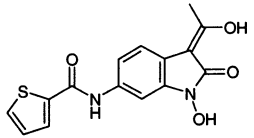
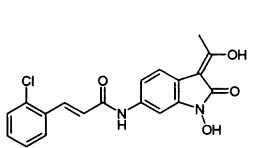
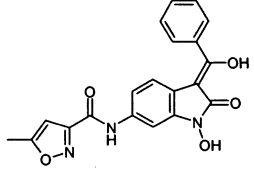
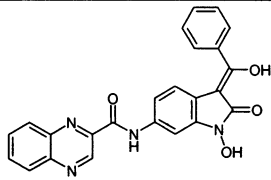
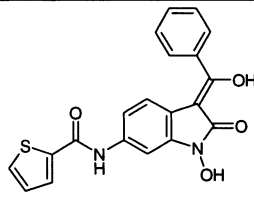
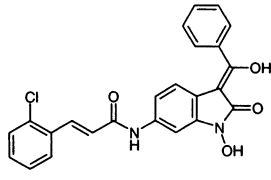
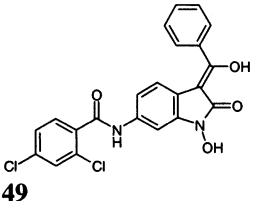
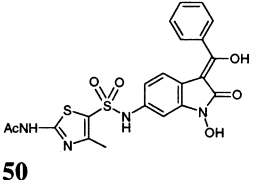
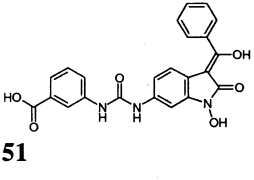
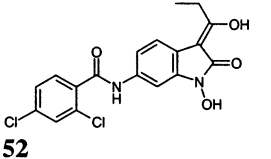
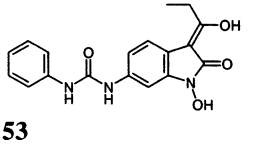
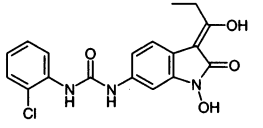
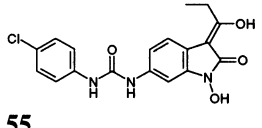
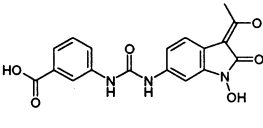
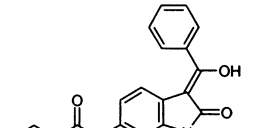
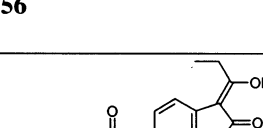
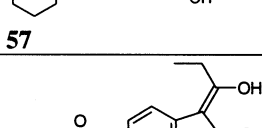
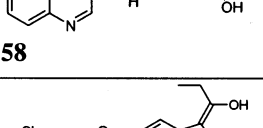
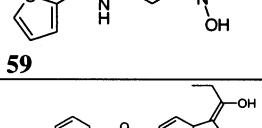
Structure	IC ₅₀ (μM) ^a A/PR/8/34	IC ₅₀ (μM) ^b B/Lee/40	EC ₅₀ (μM) ^c A/PR/8/34	Structure	IC ₅₀ (μM) ^a A/PR/8/34	IC ₅₀ (μM) ^b B/Lee/40	EC ₅₀ (μM) ^c A/PR/8/34
 36	9	18	21	 37	10	56	>90
 38	8	29	>40	 39	48	ND	ND
 40	29	ND	ND	 41	50	ND	ND
 42	11	ND	ND	 43	40	ND	ND
 44	26	ND	ND	 45	9.5	ND	>100
 46	17	ND	ND	 47	20	ND	ND
 48	9.5	26	>30	 49	38	ND	ND
 50	32	ND	ND	 51	3	6	>100
 52	45	ND	ND	 53	40	ND	ND

Table 3 (Continued)

Structure	IC ₅₀ (μM) ^a A/PR/8/34	IC ₅₀ (μM) ^b B/Lee/40	EC ₅₀ (μM) ^c A/PR/8/34	Structure	IC ₅₀ (μM) ^a A/PR/8/34	IC ₅₀ (μM) ^b B/Lee/40	EC ₅₀ (μM) ^c A/PR/8/34
 54	50	ND	ND	 55	38	ND	ND
 56	14	ND	ND	 57	18	ND	ND
 58	10	ND	ND	 59	35	ND	ND
 60	8	ND	ND	 61	10	ND	ND

^a Inhibitory potency was determined from dose response curves in cap-dependent transcription assays using RNP purified from influenza A/PR/8/34 virus. ^b RNP was from influenza B/Lee/40 virus. ^c Inhibitory potency was determined from dose response curves in antiviral assays, based on the protection of MDCK cells from influenza virus induced cell death.

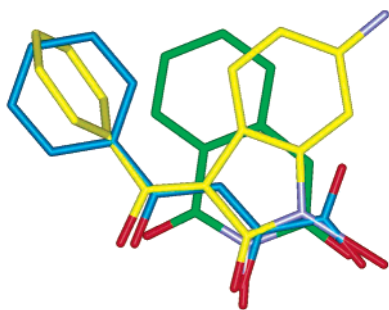


Figure 12. Modified overlay of the tetramic acid library core with 4-phenyl-2,4-diketobutanoate (**1**) and *N*-hydroxyhomophthalimide (**13**) based on the apparent preference for R¹ = Ph observed on screening the library.

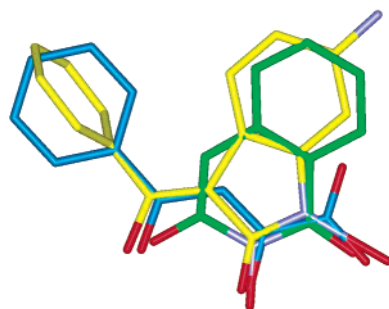


Figure 13. Alternative overlay of the tetramic acid library core with 4-phenyl-2,4-diketobutanoate (**1**) and *N*-hydroxyhomophthalimide (**13**) which is also consistent with the apparent preference for R¹ = Ph observed on screening the library.

chemical analysis of substrate cleavage and the mode of action of several series of endonuclease inhibitors. The inhibitors included in the model bind mutually exclu-

sively to the endonuclease active site. In the absence of protein structural information, the major emphasis of the current model was on compound interaction with the two catalytic metal ions in the enzyme active site in a transition state analogous fashion. Using this model we successfully designed a new class of compounds that interact with the enzyme according to our predictions.

Experimental Section

(1) Modeling. The structures used in the overlays were built and minimized in Sybyl 6.7.1 (Tripos Inc., 1699 South Hanley Rd., St Louis, MO 63144) using the Tripos force field with the default options. The structural overlays were created using a rigid fit of the key oxygens with the fit atoms function in Sybyl and the figures for this publication prepared from the resulting overlays using WebLab ViewerLite 4.0 (Accelrys Ltd., 230/250 The Quorum, Barnwell Road, Cambridge CB5 8RE, UK).

(2) Biochemistry. Cap-dependent (endonuclease dependent) influenza polymerase activity assays were run as previously described using ribonucleoprotein purified from influenza virus A/PR/8/34 and B/Lee/40.¹² Briefly, 10 nM influenza virus ribonucleoprotein (polymerase) was incubated with 50 μM GTP, 50 μM CTP, 500 μM ATP, 5 μM UTP (0.02 μCi/μL), 0.01 mg/mL AMV RNA in 50 mM Tris-HCl, pH 8, 100 mM KCl, 5 mM MgCl₂, 10% DMSO, 5 mM DTT, 0.2 mg/mL BSA on Millipore MADV 96-well filter plates. After incubation at 31 °C for 90 min, the amount of radioactive UTP incorporated into RNA transcripts was determined by precipitation of RNA with 10% trichloroacetic acid, separation of unincorporated UTP by filtration through glass fiber filters and scintillation counting. Cap-independent (endonuclease independent) influenza polymerase activity was measured using the same assay protocol, but replacing AMV RNA with 0.4 mM ApG dinucleotide in the assay.

Cap-dependent endonuclease activity assays were performed as described previously.¹² Briefly, 1 nM influenza virus ribo-

nucleoprotein was incubated with 0.1 nM cap-labeled 20-mer RNA (G20, 10000 cpm/fmol) in 50 mM Tris-HCl, pH 8, 1 mM MgCl₂, 20 mM KCl, 1 U/μL RNase inhibitor, 0.3% Triton X-100 at 31 °C for 5 min. The cleavage products were quantified after separation by electrophoresis on 20% acrylamide gels and phosphorimager scanning using ImageQuant 5.0 software. Transcription initiation reactions were performed under the same conditions by replacing the capped 20-mer RNA (G20) with the cap-labeled 11-mer RNA (G11) endonuclease product analogue. In the presence of 10 μM CTP, the 11-mer RNA is elongated by the influenza polymerase to a 12-mer RNA transcription initiation product.

(3) Chemistry. General Methods. ¹H NMR spectra were recorded at 300 MHz. The chemical shifts (δ) are expressed in ppm, and coupling constants *J* are reported in Hz. Infrared spectra were recorded using KBr pellets, and frequencies are expressed in cm⁻¹. Melting points were determined on a Büchi capillary melting point apparatus. HPLC analyses were carried out on a Develosil RP Aqueous 4.6 × 50 mm column using a gradient of 10% CH₃CN (0.5 min), 10% to 100% CH₃CN (4.5 min), and 100% CH₃CN (1 min) with a flow of 1.5 mL per min and with detection at 254 nm. The HPLC purity of the library members was found to be 85% or higher. The mass spectra of the library members were in accordance with their respective relative masses. Analytical grade reaction solvents were used as supplied with exception of THF, which was freshly distilled over potassium/benzophenone. The chloroform grade used was ethanol free and stabilized with amylene. Analytical thin-layer chromatography was performed on Merck silica gel 60F₂₅₄ plates, and flash chromatography with Merck silical gel 60 (230–400 mesh).

General Synthesis of Sulfonamides 23. To a solution of **26** (80 mg) in CHCl₃ (1.5 mL) was added pyridine (5 equiv) and 4-(dimethylamino)pyridine (10 mg) at room temperature followed by the sulfonyl chloride R²SO₂Cl (1.5 equiv) at 0 °C. The mixture was kept at room temperature for 15 h, evaporated to dryness, and submitted to chromatography to give intermediate **33**. This was dissolved in THF/MeOH (1:1, 2 mL) and treated with LiOH·H₂O (10 equiv) for 45 min at room temperature. The mixture was either treated with aqueous 1 M HCl solution (3 mL) and extracted with EtOAc, or, for substrates containing basic side chains, concentrated in vacuo and the residue was treated with aqueous phosphate buffer solution (10% NaH₂PO₄ in H₂O and addition of aqueous NaOH solution until pH 7) and extracted with CHCl₃. The organic layer was separated, dried over MgSO₄, filtered, and concentrated in vacuo. The precipitate was washed (Et₂O, pentanes) and dried in vacuo to yield the final compounds.

General Synthesis of Carboxamides 24. To a solution of **26** (80 mg) in CH₂Cl₂ (1.5 mL) was added pyridine (5 equiv) at room temperature followed by 4-(dimethylamino)pyridine (10 mg) and the acid chloride R²COCl (1.5 equiv) was added rapidly at 0 °C. The mixture was kept at room temperature for 45 min, evaporated to dryness, and submitted to chromatography to give intermediate **34**. This was dissolved in THF/MeOH (1:1, 2 mL) and treated with LiOH·H₂O (10 equiv) for 45 min. The mixture was concentrated in vacuo and treated with 1 M aqueous HCl solution (5 mL) to form a precipitate, which was filtered, washed (H₂O, Et₂O), and dried in vacuo to yield the final compounds.

General Synthesis of Ureas 25. To a solution of **26** (80 mg) in CHCl₃ (1.5 mL, ethanol free) was added the isocyanate R²NCO (1.5 equiv) at room temperature. After 2 days, the mixture was evaporated to dryness and submitted to chromatography to give intermediate **35**. This was dissolved in THF/MeOH (1:1, 2 mL) and treated with LiOH·H₂O (10 equiv) for up to 2.5 h. The mixture was concentrated in vacuo, treated with 1 M aqueous HCl solution (5 mL) to form a precipitate which was filtered, washed (H₂O, Et₂O/pentanes 1:1), and dried in vacuo to yield the final compounds.

Preparation of Building Blocks 26a, 26b, and 26c. (4-Fluoro-3-nitrophenyl)carbamic Acid *tert*-Butyl Ester (30). To a mechanically stirred, boiling solution of **29** (350.4 g, 2.24 mol) was added dropwise a solution of Boc₂O (587.6 g,

2.69 mol) in THF (350 mL). The mixture was heated under reflux overnight, and then additional Boc₂O was added in two portions (149.7 g, 686 mmol and 50 g, 229 mmol 6 h later) each in THF (100 mL). The mixture was kept under reflux overnight, and the solvent was then evaporated in vacuo. The solid residue was washed with hexanes/EtOAc 4:1, filtered, and dried to yield **30** (556.7 g, 96%) as a brownish powder. mp 115–117 °C; IR (KBr): 3363 (NH), 1702 (CO), 1549, 1520, 1323, 1284, 1240, 1159; ¹H NMR (CDCl₃) δ 1.53 (s, tBu), 6.62 (br s, NH), 7.20 (br t, *J* ~ 9.2, 1H), 7.61 (m, 1H), 8.13 (dd, *J* = 2.8, 6.3, 1H).

2-(4-*tert*-Butoxycarbonylamino-2-nitrophenyl)malonic Acid Dimethyl Ester (31). To a mechanically stirred suspension of NaH (55% in oil, 75 g, 1.72 mol, washed with hexanes) in Me₂SO (300 mL) was slowly added a solution of dimethyl malonate (200 mL, 1.74 mol) in Me₂SO (200 mL) at 15–20 °C (ice bath). The mixture was stirred for 1 h at room temperature, and then a solution of **30** (200 g, 0.78 mol) in Me₂SO (350 mL) was added over 30 min at room temperature. After stirring the reaction mixture for additional 30 min at room temperature, it was heated to 80 °C overnight, cooled to room temperature, and poured onto 2 M aqueous HCl solution/ice. The product was extracted with EtOAc, the organic layer was washed with water and brine, dried over Na₂SO₄, and concentrated in vacuo. The oily residue crystallized in the fridge overnight and was washed with hexanes/EtOAc 4:1 to give **31** (268.1 g, 93%) as a beige powder. mp 103–107 °C; IR (KBr): 3367 (NH), 1751, 1734, 1720 (CO), 1541, 1287, 1235, 1152; MS: (APCI, positive mode), *m/e* 386 (M + 18)⁺; 369 (M + 1)⁺; ¹H NMR (CDCl₃) δ 1.58 (s, tBu), 3.79 (s, 2 CH₃), 5.26 (s, 1H), 6.75 (br s, NH), 7.39 (d, *J* = 8.6, 1H), 7.58 (dd, *J* = 8.5, 2.4, 1H), 8.17 (d, *J* = 2.4, 1H).

(4-*tert*-Butoxycarbonylamino-2-nitrophenyl)acetic Acid (28). To a solution of **31** (95.2 g, 258.5 mmol) in MeOH (420 mL) was added 2 M aqueous NaOH solution (530 mL, 1060 mmol) at room temperature within 5 min. After the dark solution was heated under gentle reflux for 3 h, it was cooled in an ice bath and then added to an ice-cooled mixture of 2 M aqueous HCl solution (630 mL, 1260 mmol) and EtOAc. Extraction with EtOAc followed, and the organic layer was washed with brine until the aqueous phase showed a pH ~ 3, filtered over MgSO₄, and concentrated in vacuo to approximately 1/4 of its initial volume. It was heated for another 2 h under reflux before the solvent was removed in vacuo to give **28** (69.1 g, approximately 78%, purity (HPLC): 87%) as a pale yellow solid. A small sample was purified by flash chromatography with ethyl acetate and recrystallization from ethanol. mp 152–153 °C; IR (KBr): 3368 (NH), 2980 (br, OH), 1701 (CO), 1541, 1342, 1242, 1162; MS: (APCI, negative mode), *m/e* 295 (M - 1)⁻; ¹H NMR (CDCl₃) δ 1.54 (s, tBu), 4.00 (s, CH₂), approximately 6.9 (br s, NH), 7.26 (d, *J* = 8.4, 1H); 7.6 (br d, *J* ~ 7.3, 1H), 8.19 (d, *J* = 2.4, 1H).

2,2-Dimethylpropionic Acid 6-*tert*-Butoxycarbonylamino-2-oxo-2,3-dihydro-indol-1-yl Ester (27). A solution of **28** (23.2 g, 78.3 mmol) in EtOH (690 mL) and Me₂SO (11.6 mL) was degassed three times (vacuum/argon) at room temperature, and then 5% Pt/C (1.15 g) was added. The mixture was degassed another two times (vacuum/N₂) before the gas phase was exchanged (three times vacuum/H₂). The mixture was vigorously stirred for 23 h under H₂ (gas balloon), and then the catalyst was removed by filtration over MgSO₄/Celite. The filtrate was concentrated in vacuo to approximately 1/2 of its initial volume, AcOH (100 mL) was added at room temperature, and the resulting solution was stirred for 40 h. The solvent was evaporated in vacuo, the black tarlike residue was coevaporated twice with toluene and taken up in EtOAc. Saturated aqueous NaHCO₃ solution was added while stirring until the gas evolution stopped. The aqueous layer was extracted with EtOAc, and the combined organic layers were washed with dilute brine, filtered over MgSO₄, and concentrated in vacuo.

A suspension of the dried, crude hydroxamic acid in CH₂-Cl₂ (350 mL) was cooled in an ice bath, *N*-ethyl-diisopropylamine (15.5 mL, 90.4 mmol) was added followed by pivaloyl

chloride (9.4 mL, 76.5 mmol). The ice bath was removed after 10 min, and the mixture was stirred for 5 h at room temperature and then poured onto saturated aqueous NH₄Cl solution/EtOAc and extracted with EtOAc/Et₂O. The organic layer was washed with brine, filtered over MgSO₄, and concentrated in vacuo. Flash chromatography (gradient hexanes/EtOAc 3:1 to 2:1) yielded **27** (13.57 g, 50%) as a lilac powder. mp 158–160 °C; IR (KBr): 3366 (NH), 1788, 1744, 1723 (CO); MS: (APCI, positive mode), *m/e* 349 (M + 1)⁺; ¹H NMR (CDCl₃) δ 1.45 (s, tBu), 1.51 (s, tBu), 3.55 (s, CH₂), 6.54 (br s, NH), 6.86 (dd, *J* = 2.0, 8.0, 1H), 7.03 (br d, 1H), 7.11 (d, *J* = 8.0, 1H).

2,2-Dimethylpropionic Acid 6-tert-Butoxycarbonylamino-3-[1-acetoxylethylidene]-2-oxo-2,3-dihydroindol-1-yl Ester (32a). 4-(Dimethylamino)pyridine (0.5 g, 4.1 mmol) and *N*-ethyl-diisopropylamine (27.8 g, 215.5 mmol) were added at 0 °C to a solution of **27** (5.0 g, 14.4 mmol) in THF (100 mL). Acetic anhydride (17.6 g, 172.4 mmol) was added rapidly dropwise. The mixture was stirred for 10 min at 0 °C and an additional 3.5 h at room temperature, diluted with EtOAc (200 mL), and washed with cold, aqueous, 1 M HCl solution (3 × 200 mL), saturated aqueous NaHCO₃ solution, and brine, dried over Na₂SO₄, and concentrated in vacuo. The residue was coevaporated with toluene and dried in vacuo to give, after flash chromatography (gradient hexanes to hexanes/EtOAc 3:1), **32a** (5.22 g, 84%) as a red foam. ¹H NMR (CDCl₃) δ 1.45 (s, tBu), 1.51 (s, tBu), 2.36 (s, CH₃), 2.65 (s, CH₃), 6.57 (br s, NH), 6.84 (dd, *J* = 2.0, 8.3, 1H), 7.05 (d, *J* = 1.8, 1H), 7.37 (d, *J* = 8.3, 1H).

2,2-Dimethylpropionic Acid 6-tert-Butoxycarbonylamino-3-[1-(2,2-dimethylpropionyloxy)ethylidene]-2-oxo-2,3-dihydroindol-1-yl Ester (32a'). To a mixture of **32a** (5.2 g, 12 mmol) and NaCN (0.59 g, 12 mmol) in CH₂Cl₂ (60 mL) was added pyridine (60 mL), and it was cooled to 0 °C. Pivaloyl chloride (7.25 g, 60 mmol) was added dropwise, and the mixture was stirred for 14 h at 0 °C to 17 °C. The mixture was filtered, the filtrate diluted with EtOAc (600 mL), washed with H₂O (200 mL), cold 1 M aqueous HCl solution, saturated aqueous NaHCO₃ solution, and brine, dried over Na₂SO₄, and concentrated in vacuo. Flash chromatography (gradient hexanes to hexanes/EtOAc 3:1) afforded **32a'** (4.37 g, 76%) as a yellow foam. ¹H NMR (CDCl₃) δ 1.39 (s, tBu), 1.45 (s, tBu), 1.51 (s, tBu), 2.59 (s, CH₃), 6.55 (br s, NH), 6.92 (dd, *J* = 1.9, 8.3, 1H), 6.96 (d, *J* = 1.9, 1H), 7.45 (d, *J* = 8.3, 1H).

2,2-Dimethylpropionic Acid 6-tert-Butoxycarbonylamino-3-[1-(benzoyloxy)benzylidene]-2-oxo-2,3-dihydroindol-1-yl Ester (32b). *N*-Ethyl-diisopropylamine (1.51 g, 11.7 mmol) and 4-(dimethylamino)pyridine (70 mg, 0.57 mmol) were added at -10 °C to a solution of **27** (1.0 g, 2.87 mmol) in CH₂Cl₂/THF 2:1 (9 mL). Then a solution of benzoyl chloride (1.0 g, 7.1 mmol) in THF (3 mL) was added within 20 min at -10 °C. After 2 h at -10 °C, the mixture was poured onto 1 M aqueous HCl solution/EtOAc and extracted with EtOAc. The organic layer was washed with brine, dried over Na₂SO₄, and concentrated in vacuo. Flash chromatography (gradient hexanes/EtOAc 5:1 to 3:1) afforded **32b** (1.0 g, 62%). ¹H NMR (CDCl₃) δ 1.42 (s, tBu), 1.49 (s, tBu), 6.57 (br s, 1H), 6.75 (dd, *J* = 2.1, 8.4, 1H), 7.04 (d, *J* = 1.9, 1H), 7.38–7.77 (m, 9H), 8.19–8.22 (m, 2H).

2,2-Dimethylpropionic Acid 6-tert-Butoxycarbonylamino-3-[1-(propionyloxy)propylidene]-2-oxo-2,3-dihydroindol-1-yl Ester (32c). To a 0 °C cooled solution of **27** (4.95 g, 14.2 mmol) in THF/CH₂Cl₂ 1:2 (85 mL) was added *N*-ethyl-diisopropylamine (12.8 g, 99.3 mmol) followed by 4-(dimethylamino)pyridine (0.35 g, 2.9 mmol). A solution of propionyl chloride (6.56 g, 71 mmol) in CH₂Cl₂ (30 mL) was added over a period of 20 min. The mixture was stirred for 2.5 h at 0 °C and then diluted with EtOAc and aqueous 1 M HCl solution. The organic layer was separated, washed (aqueous 1 M HCl solution, H₂O, brine), dried over Na₂SO₄, and concentrated in vacuo. Flash chromatography (gradient hexanes/EtOAc 5:1 to 3:1) afforded **32c** (4.8 g, 73%) as a brown foam. MS: (APCI, positive mode), *m/e* 387 (M - OPiv)⁺; ¹H NMR (CDCl₃) δ 1.16 (t, *J* = 7.5, CH₃), 1.30 (t, *J* = 7.5, CH₃), 1.45 (s, tBu), 1.51 (s, tBu), 2.68 (q, *J* = 7.5, CH₂), 3.21 (q, *J* = 7.5, CH₂), 6.55 (br s,

NH), 6.85 (dd, *J* = 2.0, 8.3, 1H), 7.02 (d, *J* = 1.9, 1H), 7.34 (d, *J* = 8.3, 1H).

2,2-Dimethylpropionic Acid 6-tert-Butoxycarbonylamino-3-[1-(2,2-dimethylpropionyloxy)propylidene]-2-oxo-2,3-dihydroindol-1-yl Ester (32c'). A solution of Bu₄NCN (21 mg) in CH₂Cl₂ (3 mL) was added to a 0 °C cooled solution of **32c** (3.0 g, 6.5 mmol) in CH₂Cl₂/pyridine 1:1 (72 mL). Pivaloyl chloride (7.9 g, 65.8 mmol) was added within 2 min, and the mixture was stirred for 20 min at 0 °C and 16 h at room temperature. The mixture was poured onto EtOAc/aqueous 1 M HCl solution, the organic layer was separated, washed (aqueous 1 M HCl solution, H₂O, saturated aqueous NaHCO₃ solution, brine), dried over Na₂SO₄, and concentrated in vacuo. Flash chromatography (gradient hexanes/EtOAc 7:1 to 4:1) afforded **32c'** (2.07 g, 65%). ¹H NMR (CDCl₃) δ 1.17 (t, *J* = 7.5, CH₃), 1.42 (s, tBu), 1.45 (s, tBu), 1.51 (s, tBu), 3.17 (q, *J* = 7.5, CH₂), 6.60 (br s, NH), 6.90–6.95 (m, 2H), 7.43 (d, *J* = 8.6, 1H).

2,2-Dimethylpropionic Acid 6-Amino-3-[1-(2,2-dimethylpropionyloxy)ethylidene]-2-oxo-2,3-dihydroindol-1-yl Ester (26a). To neat **32a'** (3.93 g, 8.3 mmol) was added 4 M HCl in dioxane (30 mL) at room temperature while stirring. After 75 min it was poured onto a mixture of EtOAc (100 mL)/saturated aqueous NaHCO₃ solution (200 mL). The organic layer was separated, washed with brine, dried over Na₂SO₄, and concentrated in vacuo. The crude product was treated with Et₂O/hexanes 2:3 to give a precipitate which was filtered and dried in vacuo to yield **26a** (2.20 g, 71%) as a green powder. The filtrate was concentrated in vacuo and purified by flash chromatography (gradient hexanes/EtOAc 7:3 to 3:2) to give additional **26a** (0.3 g, 9%). ¹H NMR (CDCl₃) δ 1.39 (s, tBu), 1.44 (s, tBu), 2.55 (s, CH₃), 3.85 (br s, NH₂), 6.02 (d, *J* = 2.1, 1H), 6.30 (dd, *J* = 2.1, 8.2, 1H), 7.33 (d, *J* = 8.2, 1H).

2,2-Dimethylpropionic Acid 6-Amino-3-[1-(benzoyloxy)benzylidene]-2-oxo-2,3-dihydroindol-1-yl Ester (26b). To neat **32b** (1.0 g, 1.8 mmol) was added ice cold 4 M HCl in dioxane (6 mL). The mixture was stirred for 1.5 h at room temperature and then poured onto a mixture of ice, saturated aqueous NaHCO₃ solution, and EtOAc. Extraction with EtOAc followed, and the organic layer was washed with brine, dried (Na₂SO₄), and concentrated in vacuo. The crude product was suspended in Et₂O/hexanes 2:1, and the resulting precipitate was filtered and dried in vacuo to yield **26b** (605 mg, 73%). mp 190–193 °C; IR (KBr): 3446, 3360 (NH), 1790, 1743, 1720 (CO), 1639; ¹H NMR (Me₂SO-*d*₆) δ 1.34 (s, tBu), 5.85 (s, exchanged with D₂O, NH₂), 6.10–6.13 (m, 2H), 7.07 (d, *J* = 8.2, 1H), 7.36–7.89 (m, 8H), 8.18 (d, *J* ~ 8.4, 2H).

2,2-Dimethylpropionic Acid 6-Amino-3-[1-(2,2-dimethylpropionyloxy)ethylidene]-2-oxo-2,3-dihydroindol-1-yl Ester (26c). To neat **32c'** (3.7 g, 7.6 mmol) was added 4 M HCl in dioxane (37 mL) at room temperature while stirring. A precipitation was formed, and after 75 min the mixture was concentrated in vacuo. The residue was suspended in absolute Et₂O (30 mL), stirred for 15 min, treated with hexanes (45 mL), and filtered. The residue was washed (hexanes) and dried in vacuo to yield **26c**·HCl (2.68 g, 83%) as a lightweight powder. ¹H NMR (Me₂SO-*d*₆) δ 1.08 (t, *J* = 7.5, CH₃), 1.37 (s, 2 tBu), 3.00 (br s, 2H), approximately 6.3 (very br s), 6.36 (br s, 1H), 6.55 (br d, 1H), 7.24 (d, *J* = 8.3, 1H).

An analytical sample of **26c**·HCl was dissolved in EtOAc and treated with saturated aqueous Na₂CO₃ solution. The organic layer was separated, filtered over MgSO₄, and concentrated in vacuo. Flash chromatography (gradient hexanes/EtOAc 3:1 to 2:1) afforded **26c**. IR (KBr): 3377 (NH), 2976, 1796, 1718 (CO), 1631, 1065; MS: (APCI, positive mode), *m/e* 389 (M + 1)⁺, 287; ¹H NMR (Me₂SO-*d*₆) δ 1.06 (br t, CH₃), 1.35–1.37 (m, 18H, 2 tBu), 2.93 (br s, CH₂), 5.71 (br s, NH₂), 6.06 (s, 1H), 6.24 (d, *J* = 8.2, 1H), 7.09 (d, *J* = 8.2, 1H).

Specific Examples. 3-{3-[1-Hydroxy-3-(1-hydroxybenzylidene)-2-oxo-2,3-dihydro-1*H*-indol-6-yl]ureido}-benzoic Acid (51). According to general procedure: powder, 56 mg (74%). mp 203 °C (dec); IR (KBr): 3377 (br, NH, OH), 1627 (CO), 1554; HPLC: *t*_R = 4.23 min, 93% purity; mass (APCI, positive mode), *m/e* 432 (M + 1)⁺; ¹H NMR (Me₂SO-*d*₆)

δ 6.73–6.92 (m, 2H, partial exchange with D₂O), 7.30–7.75 (m, 10H), 8.10 (s, 1H), 8.92 (br s, 2H, exchange with D₂O), 11.14 (br s, 1H, exchange with D₂O), 12.87 (br s, exchange with D₂O).

Naphthalene-2-carboxylic Acid [1-Hydroxy-3-(1-hydroxyethylidene)-2-oxo-2,3-dihydro-1H-indol-6-yl]-amide (36). According to general procedure: powder, 47 mg (61%); mp 175–183 °C (dec); IR (KBr): 3406 (br, NH, OH), 1660 (CO), 1530; HPLC: t_R = 4.51 min, 89% purity; MS: (ESI, negative mode), m/e 359 (M – 1)⁻; ¹H NMR (Me₂SO-*d*₆) δ 2.44 (s, CH₃ minor isomer), 2.56 (s, CH₃ major isomer), 7.35–7.56 (m, 5H), 7.98–8.08 (m, 4H), 8.57 (s, 1H), 10.37 (s, 2H, exchange with D₂O).

N-{5-[1-Hydroxy-3-(1-hydroxybenzylidene)-2-oxo-2,3-dihydroindol-6-ylsulfamoyl]-4-methylthiazol-2-yl}-acetamide (50). According to general procedure: yellowish solid, 37 mg (43%); HPLC: t_R = 4.33 min, 95% purity; MS: (APCI, negative mode), m/e 485 (M – 1)⁻; ¹H NMR (Me₂SO-*d*₆) δ 2.12 (s, CH₃), 2.34 (s, CH₃), 6.67–6.92 (m, 3H, after addition of D₂O 2H), 7.45–7.93 (m, 7H, after addition of D₂O 6H), 10.53 (s, 0.5H, exchange with D₂O), 11.19 (s, 0.5H, exchange with D₂O), 12.46 (s, 1H, exchange with D₂O).

Acknowledgment. We would like to thank Professor Andrea Vasella (ETH, Zurich) for helpful discussions on potential structures matching the pharmacophore, Linh Doan and Lisa Hooker for excellent technical assistance, and Professor John Bol, Lyda Neeleman, and Frans Brederode for their support in RNA production.

Supporting Information Available: A table showing the composition of the tetramic acid library. This material is available free of charge via the Internet at <http://pubs.acs.org>.

References

- (1) (a) Sherif, B.; Mossad, M. D. Prophylactic and symptomatic treatment of influenza. *Postgrad. Med.* **2001**, *109*, 97–105. (b) Cram, P.; Blitz, S. G.; Monto, A.; Fendrick, A. M. Cost of illness and considerations in the economic evaluation of new and emerging therapies. *Pharmacoeconomics* **2001**, *19*, 223–230. (c) Cox, N. J.; Subbarao, K. Influenza. *Lancet* **1999**, *354*, 1277–1282. (d) Luo, G.; Cianci, C.; Harte, W.; Krystal, M. Conquering Influenza: Recent advances in anti-influenza drug discovery. *IDrugs* **1999**, *2*, 671–685 (e) Cianci, C.; Krystal, M. Development of antivirals against influenza. *Exp. Opin. Invest. Drugs* **1998**, *7* (2), 149–164. (f) Colacino, J. M.; Staschke, K. A.; Laver W. G. Approaches and Strategies for the treatment of influenza virus infections. *Antiviral Chem. Chemother.* **1999**, *10*, 155–185. (g) Meanwell, N. A.; Krystal, M. Taking aim at a moving target – inhibitors of influenza virus Part 1: virus adsorption, entry and uncoating. *Drug Discovery Today* **1996**, *1* (8), 316–324. Part 2: viral replication, packaging and release. *Drug Discovery Today* **1996**, *1* (8), 388–397.
- (2) (a) Lamb, R. A.; Krug, R. M. Orthomyxoviridae: the viruses and their replication. In *Virology*, 3rd ed.; Fields, B. N., Knipe, D. M., Howley, P. M., Eds.; Lippincott-Raven Publishers: Philadelphia, 1996; pp 1353–1395. (b) Honda, A.; Ishihama, A. The Molecular Anatomy of Influenza Virus RNA Polymerase. *Biol. Chem.* **1997**, *378*, 483–488.
- (3) (a) Li, M.-L.; Rao, P.; Krug, R. M. The active sites of the influenza cap-dependent endonuclease are on different polymerase subunits. *EMBO* **2001**, *20* (8), 2078–86. (b) Doan, L.; Handa, B.; Roberts, N. A.; Klumpp, K. Metal Ion Catalysis of RNA Cleavage by the Influenza Virus Endonuclease. *Biochemistry* **1999**, *38*, 5612–9.
- (4) (a) Raines, R. T. Ribonuclease A. *Chem. Rev.* **1998**, *98*, 1045–1065. (b) Zegers, I.; Loris, R.; Dehollander, G.; Haikal, A. F.; Poortmans, F.; Steyaert, J.; Wyns, L. Hydrolysis of a slow cyclic thiophosphate substrate of RNase T1 analysed by time-resolved crystallography. *Nat. Struct. Biol.* **1998**, *5*, 280–283.
- (5) (a) Suck, D.; Oefner, C. Structure of DNase I at 2.0 Å resolution suggests a mechanism for binding to and cutting DNA. *Nature* **1986**, *321*, 620–625. (b) Weston, S. A.; Lahm, A.; Suck, D. X-ray structure of the DNase I–d(GGTATACC)₂ complex at 2.3/ resolution. *J. Mol. Biol.* **1992**, *226*, 1237–1256. (c) Galburt, E. A.; Chevalier, B.; Tang, W.; Jurica, M. S.; Flick, K. E.; Monnat, R. J., Jr.; Stoddard, B. L. A novel endonuclease mechanism directly visualized for I–PpoI. *Nat. Struct. Biol.* **1998**, *6*, 1096–1099. (d) Miller, M. D.; Cai, J.; Krause, K. L. The active site of Serratia endonuclease contains a conserved magnesium-water cluster. *J. Mol. Biol.* **1999**, *288*, 975–987.
- (6) (a) Beese, L. S.; Steitz, T. A. Structural basis for the 3′–5′ exonuclease activity of *Escherichia coli* DNA polymerase I: a two metal ion mechanism. *EMBO J.* **1991**, *10*, 25–33. (b) Kim, E. E.; Wyckoff, H. W. Reaction mechanism of alkaline phosphatase based on crystal structures. *J. Mol. Biol.* **1991**, *218*, 449–464. (c) Horton, J. R.; Cheng, X. PvuII endonuclease contains two calcium ions in active sites. *J. Mol. Biol.* **2000**, *300*, 1049–1056. (d) Xu, R. X.; Hassell, A. M.; Vanderwall, D.; Lambert, M. H.; Holmes, W. D.; Luther, M. A.; Rocque, W. J.; Milburn, M. V.; Zhao, Y.; Ke, H.; Nolte, R.; T. Atomic structure of PDE4: insights into phosphodiesterase mechanism and specificity. *Science* **2000**, *288*, 1822–1825. (e) Steitz, T. A. DNA polymerases: structural diversity and common mechanisms. *J. Biol. Chem.* **1999**, *274*, 17395–17398.
- (7) Tomassini, J.; Selnick, H.; Davies, M. E.; Armstrong, M. E.; Baldwin, J.; Bourgeois, M.; Hastings, J.; Hazuda, D.; Lewis, J.; McClements, W.; Ponticello, G.; Radzilowski, E.; Smith, G.; Tebben, A.; Wolfe, A. Inhibition of Cap (m7GpppXm)-Dependent Endonuclease of Influenza Virus by 4-substituted 2,4-Dioxobutanoic Acid Compounds. *Antimicrob. Agents Chemother.* **1994**, *38* (12), 2827–37.
- (8) Hastings, J. C.; Selnick, H.; Wolanski, B.; Tomassini, J. E. Anti-Influenza Virus Activities of 4-Substituted 2,4-Dioxobutanoic Acid Inhibitors. *Antimicrob. Agents Chemother.* **1996**, *40* (5), 1304–7.
- (9) (a) Tomassini, J. E.; Davies, M. E.; Hastings, J. C.; Lingham, R.; Mojena, M.; Raghoobar, S. L.; Singh, S. B.; Tkacz, J. S.; Goetz, M. A. A Novel Antiviral Agent Which Inhibits the Endonuclease of Influenza Viruses. *Antimicrob. Agents Chemother.* **1996**, *40* (5), 1189–1193. (b) Hensens, O. D.; Goetz, M. A.; Liesch, J. M.; Zink, D. L.; Raghoobar, S. L.; Helms, G. L.; Singh, S. B. Isolation and Structure of Flutimide, a Novel Endonuclease Inhibitor of Influenza Virus. *Tetrahedron Lett.* **1995**, *36* (12), 2005–8.
- (10) Singh, S. B. Total Synthesis of Flutimide, A Novel Endonuclease Inhibitor of Influenza Virus. *Tetrahedron Lett.* **1995**, *36* (12), 2009–2012. (b) Singh, S. B.; Tomassini, J. E. Synthesis of Natural Flutimide and Analogous Fully Substituted Pyrazine-2,6-diones, Endonuclease Inhibitors of Influenza Virus. *J. Org. Chem.* **2001**, *66*, 5504–5516.
- (11) Cianci, C.; Chung, T. D. Y.; Meanwell, N.; Putz, H.; Hagen, M.; Colonna, R. J.; Krystal, M. Identification of N-hydroxamic acid and N-hydroxyimide compounds that inhibit the influenza virus polymerase. *Antiviral Chem. Chemother.* **1996**, *7* (6), 353–60.
- (12) Klumpp, K.; Hooker, L.; Handa, B. Influenza virus endonuclease. *Methods Enzymol.* **2001**, *342*, 451–466.
- (13) Kees, K. L.; Caggiano, T. J.; Steiner, K. E.; Fitzgerald, J. J.; Kates, M. J.; Christos, T. E.; Kulishoff, J. M.; Moore, R. D.; McCaleb, M. L. Studies on New Acidic Azoles as Glucose-Lowering Agents in Obese, Diabetic db/db Mice. *J. Med. Chem.* **1995**, *38*, 617.
- (14) Ames, G. N-Hydroxy-imides. Part II Derivatives of Homophthalic and Phthalic Acids. *J. Chem. Soc.* **1955**, 3518.
- (15) Wright, W. B.; Collins, K. H. Cyclic Hydroxamic Acids Derived from Indole. *J. Am. Chem. Soc.* **1956**, *78*, 221–224.
- (16) Kende, A. S.; Thurston, J. Synthesis of 1-Hydroxyoxindoles. *Synth. Commun.* **1990**, *20*, 2133–2138.
- (17) Segel, I. H. In *Enzyme Kinetics*; Wiley Classics Library Edition 1993, John Wiley and Sons Inc.: New York, 1993.

JM020334U